A CONTINUUM MODEL ACCOUNTING FOR THE EFFECT OF THE INITIAL AND EVOLVING MICROSTRUCTURE ON THE EVOLUTION OF DYNAMIC RECRYSTALLIZATION

HARM KOOIKER[†*], EMIN S. PERDAHCIOĞLU[†] AND TON VAN DEN BOOGAARD[†]

[†] Department of Nonlinear Solid Mechanics
University of Twente
Drienerlolaan 5, 7522 NB Enschede, the Netherlands

[*]Philips Consumer Lifestyle
Amstelplein 2, 1096 BC, Amsterdam
e-mail: harm.kooiker@philips.com

Key words: Dynamic Recrystallization, Grain Size, Microstructure, Constitutive Modeling

Abstract. Laser assisted forming is a process which is increasingly being adopted by the industry. Application of heat by a laser to austenitic stainless steel (ASS) sheet provides *local* control over formability and strength of the material. The hot forming behavior of ASS is characterized by significant dynamic recovery and dynamic recrystallization. These two processes lead to a softening stress-strain response and have a significant impact on the microstructure of the material. Most of the research performed on hot forming of ASS focuses on dynamic recrystallization and then specifically on the behavior of the annealed state, consisting of relatively large equiaxed austenite grains. However, in industry it is common to use cold rolled ASS sheet which is a mixture of austenite and martensite. Application of a laser heat treatment to the cold rolled grades of ASS induces a so-called 'reverse' transformation of martensite to austenite which, depending on the exact time-temperature combinations, leads to an austenite grain size in the range of nano-to micrometer. It is known from experiments that the effect of initial grain size on dynamic recrystallization is significant, especially on the initial stages of recrystallization. Therefore any continuum model capable of describing hot forming of cold rolled ASS should include the effect of the initial grain size.

In this work a physically based continuum model for dynamic recrystallization is presented which accounts for the effect of the initial *and* evolving grain size on the evolution of dynamic recrystallization. It is shown that the initial grain size can be accounted for by incorporating its effect on the availability of preferred nucleation sites, i.e. grain edges. The new model is compared to experimental results and it is shown that the model correctly predicts accelerated recrystallization with decrease in grain size and that

there is a weak dependence of the dynamically recrystallized grain size on the initial grain size. Furthermore predicted recrystallized grain sizes are in good agreement with the experimentally measured values.

1 INTRODUCTION

Metastable austenitic stainless steels (ASS) are widely used in industry due to their excellent corrosion resistance and formability. When designing products from ASS a designer must adhere to the current trade-off between hardness and ductility, where high hardness is usually required for product performance and ductility is required for make-ability, the latter limiting the attainable functional hardness of the product. Recently, there is an increased focus on laser assisted forming of ASS to enable local control of strength and formability. During this high temperature forming of ASS, dynamic recovery and dynamic recrystallization takes place leading to significant stress softening and a steady state stress lower than the peak stress [1, 2].

In industry it is common to use cold-rolled grades of ASS to achieve the desired overall functional hardness. The cold rolled grades are a mixture of austenite and martensite due to the mechanically induced transformation during rolling. When they are exposed to a heat treatment, such as during laser assisted forming, the martensite can revert back to finely grained austenite [3–5]. Numerous experimental results show that the initial grain size has a significant effect on the onset and progression of recrystallization [1,6,7] because of the dependence of potential nucleation sites on the grain size [8]. Another important observation is the weak to non-existent dependence of the steady state grain size on the initial grain size where it is found that deformation conditions are leading.

To be able to design optimal and safe products and first-time-right processes, it is imperative to have accurate quantitative models with which the process *and* product performance can be predicted up-front. The functional strength of a laser assisted forming zone *after* forming (and cooling down) is dependent on the grain size evolution during the transient hot forming process. Therefore a proper continuum mechanical description of the hot forming behavior of ASS should be able to account for the effect of initial *and* evolving grain size.

In [9] the authors have presented a physically based continuum model to predict the hot forming behavior of austenitic stainless steel at a range of high temperatures and strain rates. In this paper this model is adapted to be able to predict the effect of initial *and* evolution of austenitic grain size on the dynamic recrystallization and stress-softening behavior. The adapted model is fitted to the experimental results of Wahabi et al. [7] and it is shown that it is capable of accounting for the effect of initial grain size on the progression of dynamic recrystallization and that there is a good match between the predicted and reported grain sizes.

2 MODELING OF HOT FORMING

In this section, for sake of clarity, the complete model is highlighted, however the novelty of the current work lies in the treatment of the effect of grain size on the *recrystallization* behavior. To model the hot forming behavior of austenitic stainless steel we employ the Bergström equation [10] and assume that the behavior can be modeled by properly accounting for the effect of several mechanisms on one internal variable, i.e. the average density of immobile dislocations (henceforth dislocation density). The mechanisms included in this work are dynamic recovery, dynamic recrystallization (and the effect of grain size on this behavior) and grain boundary strengthening.

$$\sigma_y = \sigma_i + \sigma_w + \frac{k_d}{\sqrt{D}} \tag{1}$$

In which σ_i and σ_w is the frictional stress and work hardening stress respectively and $\frac{k_d}{\sqrt{D}}$ represents the Hall-Petch effect accounting for grain boundary strengthening. The Taylor equation is now employed for the relation between work-hardening and dislocation density.

$$\sigma_w = \alpha \mu b M \sqrt{\rho} \tag{2}$$

Dynamic recrystallization is modeled by incorporating it as a time-dependent factor in the Bergström work hardening equation.

$$d\rho = (h\sqrt{\rho} - f\rho)d\varepsilon - \frac{dR}{dt}(\rho - \rho_0)dt \tag{3}$$

Here $h\sqrt{\rho}$ describes the hardening by immobilization of dislocations and is inversely proportional to the mean free path of dislocations, f describes the annihilation and remobilization of immobile dislocations by dynamic recovery and $\frac{dR}{dt}$ is the time dependent dynamic recrystallization term.

In previous research, it was shown that annealed austenitic stainless steel tends to form subgrains after some deformation and that this significantly affects the mean free path [11]. In order to be able to accommodate this changing mean free path the following evolution equation for the hardening parameter is adopted [12]:

$$\frac{dh}{d\varepsilon} = \frac{K}{\sqrt{\rho}}(h_s - h) \tag{4}$$

Where K describes the rate at which the substructure is formed and h_s is the saturation value of the hardening parameter.

2.1 Dynamic recrystallization and the effect of grain size

Discontinuous dynamic recrystallization is a process governed by nucleation and growth. During dynamic recrystallization new grains nucleate and consume highly dislocated grains replacing it with new grains of relatively low dislocation density. As the hot deformation process proceeds the new grains can harden to the point where they themselves

can be consumed by yet new grains. The continuous nucleation and growth process leads to a distribution of recrystallizing grains continuously replacing the concurrently hardening material. At the steady state stress there is a balance between new nucleation, growth of previously nucleated grains and impingement of grains that thus cannot grow further and therefore the distribution will remain constant, see Figure 1. Note that this does not mean that recrystallization is finished. It means that the recrystallization *rate* at the steady state is constant and therefore the recrystallized fraction can exceed 100%. In [9] it was shown that it is possible to accurately describe the effect of recrystallization on the stress–strain behavior by modeling the volume consumption of an assembly of N grains of average diameter $\bar{D}_r$ as a representative of the volume consumption of the distribution of recrystallizing grains.

$$\frac{dR}{dt} = \pi N \bar{D}_r{}^2 \bar{v} + \frac{1}{6}\pi \frac{dN}{dt} \bar{D}_r{}^3 \tag{5}$$

Where N is the amount of recrystallizing grains of average size $\bar{D}_r$ and $\bar{v}$ is the grain boundary migration speed. To complete this model a relation is needed to describe the evolution of the average grain size and the amount of recrystallizing grains of this average size, i.e. $\frac{d\bar{D}_r}{dt}$ and $\frac{dN}{dt}$ respectively. The novelty of the current work lies in the definition of these two evolution laws by incorporating the effect of grain size.

To include the effect of grain size on recrystallization it is proposed to couple the net nucleation of grains *and* growth of the average grain size to the availability of preferred nucleation sites like grain junctions, edges or surfaces. Though it is likely that more than one type of nucleation site will be(come) active throughout a hot deformation process, here it is assumed that recrystallization can be described by properly modeling the dominant nucleation site, i.e. grain edge. Note that *net* nucleation means that it represents both new nucleation and impingement, i.e. at the steady state there is a constant distribution and thus no net nucleation.

Available edge length

The availability of grain edges for net nucleation is determined by comparing the currently occupied grain edge L_{oc} to the available grain edge L_{av}. The available grain edge depends on the current grain size of the material, i.e. D_a which, depending on the extent of recrystallization, is a mix of the initial grains and recrystallizing grains $\bar{D}_r$, see Eq. 11. The amount of grain edge available for nucleation is determined by assuming that a representative volume is filled homogeneously by cubes of size D_a. It is clear that a cube is a simplification of the actual grain shape, however it is expected that the functional dependence of the explicit relations derived below will be similar for other grain shapes. The cube-approach has the distinct advantage of being easy to visualize. Every cube of size D_a has 12 edges and every edge is shared by 4 neighbors, therefore the amount of edge per unit volume can be described by:

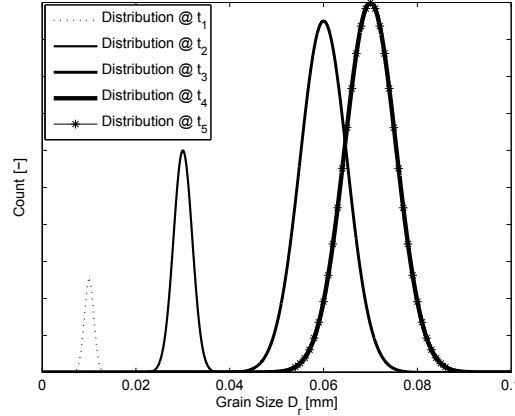$$L_{av} = (12/4)D_a N_{max} = 3D_a \left(\frac{1}{D_a}\right)^3 \tag{6}$$

Figure 1: Change of the distribution of recrystallizing grains ($t_1 < t_2 < t_3 < t_4 < t_5$), at the steady state the distribution is constant (compare t_4 and t_5), i.e. nucleation and impingement cancel and the average of the grain size remains constant

Occupied edge length

To determine the occupation of grain edge by the assembly of recrystallizing grains it is important to account for the relative size of the recrystallizing grains $\bar{D}_r$ versus the current average grain size D_a. For average recrystallizing grain sizes above $\frac{1}{2}D_a$ the occupied grain edge is simply the amount of D_a grains encompassed by $\bar{D}_r$ grains times the grain edge of a D_a-grain ($3D_a$). For grain sizes smaller than $\frac{1}{2}D_a$ the occupied grain edge length is determined by looking at the amount of $\bar{D}_r$-grains that can fit on the perimeter of a D_a-grain. A D_a grain has 12 edges and 8 corners, every edge can house ($\frac{D_a}{D_r} - 2$) grains. This leads to the following conditional relation for the *average* occupied edge length:

$$L_{oc} = \begin{cases} \dfrac{3ND_a}{8 + 12(\frac{D_a}{D_r} - 2)}, & \text{if } \bar{D}_r \leq .5D_a \\ 3ND_a\big(\frac{\bar{D}_r}{D_a}\big)^3, & \text{if } \bar{D}_r > .5D_a \end{cases} \tag{7}$$

This relation converges to the appropriate edge consumption for $\bar{D}_r << D_a$ being $\frac{1}{4}\bar{D}_r$ and to $\frac{3}{4}\bar{D}_r$ for $\bar{D}_r = 0.5D_a$.

Note that this type of nucleation and growth dependence makes it possible to describe the necklacing behavior seen in many experiments [7, 13–15] and which has a significant effect on the recrystallization evolution. The principle of necklacing is explained in 2D in Figure 2(a-b) and shown in a micrograph in Figure 2(c). If the recrystallizing grain size is small compared to the average size of the grains $\bar{D}_r << D_a$ a necklace of small grains will be formed along the grain edge. The interior of the large grains can only be recrystallized *after* they are reached by subsequent necklaces and grain edge becomes locally available. From a recrystallization viewpoint necklacing serves to delay the peak of recrystallization due to the fact that initially, depending on the ratio $\bar{D}_r$ and D_a, only a small portion of the volume *can* be recrystallized.
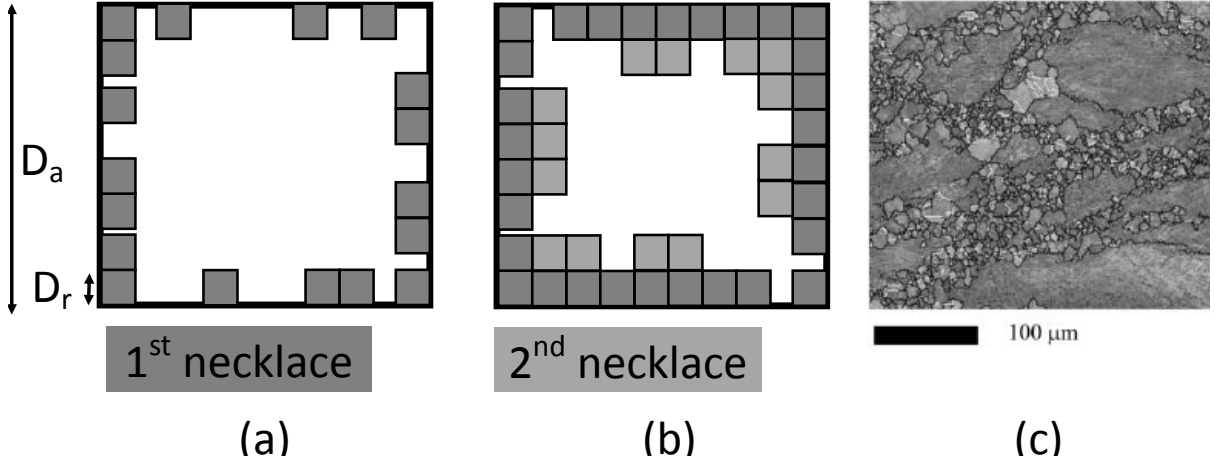
Figure 2: Explanation of a necklacing recrystallization sequence in *one* D_a-grain with a corresponding micrograph [7] displaying the phenomenon in the 92 µm experiments modeled in this paper

The derived formulations for the available and occupied edge length can now be implemented into the evolution equations for the average recrystallizing grain size $\frac{d\bar{D}_r}{dt}$ and number of recrystallizing grains $\frac{dN}{dt}$.

Average size of recrystallizing grains

The average size of the assembly of recrystallizing grains is determined by three mechanisms: nucleation, growth and impingement. Nucleation proportionally lowers the average size of the recrystallizing grains towards the size of the nuclei ($\bar{D}_{r_0}$). Growth enlarges the average size of the assembly with the average grain boundary migration speed $\bar{v}$. However growth cannot continue unbounded, i.e. growth stops when the occupied edge length equals the available edge length.

$$\frac{d\bar{D}_r}{dt} = 2\bar{v}\Big(1 - \frac{L_{oc}}{L_{av}}\Big) - (\bar{D}_r - \bar{D}_{r_0})\frac{1}{N}\frac{dN}{dt} \tag{8}$$

The term $\big(1 - \frac{L_{oc}}{L_{av}}\big)$ represents the lack of growth space for the growing grains. It is implicitly assumed that they remain equiaxed and do not bulge into the interior of the grain. This is in line with the frequently reported equiaxed recrystallization structures found in experiments [16]. The grain boundary migration speed is derived from the pressure on the boundary P and the grain boundary mobility m [8].

$$\bar{v} = mP = m\frac{1}{2}\mu b^2 \rho \tag{9}$$

Table 1: Material, chosen and optimized parameters

α	0.5	$\bar{D}_{r0}$	$1 \cdot 10^{-3}$ mm	f	7.3	m	$9.9 \cdot 10^{-5}$ mm^4/Js
μ	$4.6 \cdot 10^4$ N/mm^2	ρ_0	$2.0 \cdot 10^4$ mm^{-2}	K	$1.6 \cdot 10^5$ mm^{-1}		
b	$2.8 \cdot 10^{-7}$ mm	h_0	$1.5 \cdot 10^6$ mm^{-1}	k_d	1.2 N/mm$^{3/2}$		
M	3	h_s	$5.2 \cdot 10^4$ mm^{-1}	c_n	$2.5 \cdot 10^5$ (Nm)$^{-1}$		

Number of recrystallizing grains

The nucleation of new grains into the assembly of grains of average size $\bar{D}_r$ depends on the available driving force P and availability of nucleation sites $\left(1 - \frac{L_{oc}}{L_{av}}\right)$.

$$\frac{dN}{dt} = c_n\left(1 - \frac{L_{oc}}{L_{av}}\right)P = c_n\left(1 - \frac{L_{oc}}{L_{av}}\right)P \tag{10}$$

Where c_n is the proportionality between the driving force and nucleation rate. The last equation that is needed is a relation between the change in the average size, the size of the recrystallizing grains and the ongoing recrystallization, i.e. when the materials recrystallizes the old (*initial*) grains of size D_0 are replaced by new grains of size $\bar{D}_r$. It is assumed that D_a is completely represented by $\bar{D}_r$ when the entire material has been recrystallized i.e. $R > 1$.

$$D_a = D_0\left(1 - F(R)\right) + D_r F(R) \tag{11}$$

Here F is a sigmoid function which, depending on R, ranges from zero to one, representing the smooth transition from D_0 to $\bar{D}_r$ from $R = 0$ to $R \geq 1$.

3 RESULTS

The proposed model is fitted to the data presented by Wahabi et al. who performed hot compression experiments on highly pure austenitic stainless steel of varying initial grain size (10, 24 and 92 µm). The material can be considered a model material for commercially available AISI-304 in regards to nickel and chrome content, but has a very low amount of interstitial elements. The experiments that were modeled were performed at 850°C and a strain rate of 0.001 s^{-1}. The model has in total 13 parameters of which 8 were fitted, 4 are material parameters and one was selected (respectively α, μ, b, M and the nucleus size $\bar{D}_{r0}$). The fitting was done by least squares optimization and the set of best fitting parameters is presented in Table 1. The results of the model are presented in Figure 3. Note that the entire recrystallization behavior is represented by only two parameters, the grain boundary mobility m and the nucleation proportionality c_n.

4 DISCUSSION AND CONCLUSION

The experiments of Wahabi et al. depicted in Figure 3(a) show that the smaller grain size materials display a pronounced softening whereas the large grain material does not

show softening. In the same graph, the results of the model are in very good agreement with the experimental results. Clearly the observed softening, and its grain size dependence, can be described by using only two parameters for recrystallization supplemented with the proposed explicit relations for edge availability and occupation. For the larger grain material (92 µm) the stress–strain curve seems hardly affected by recrystallization, although the micrograph in Figure 2(c) made after the experiment does show a significant amount of small recrystallized grains arranged in necklace formation along the perimeter of large grains. Figure 3(b) and 3(c) show that the model closely matches this observation with the prediction of a significant amount of small recrystallizing grains, yet without having much effect on the stress–strain response. In Figure 3(c) the evolution of the amount of grains for the largest grain size (92 µm) displays a plateau, indicating that the occupied grain edge equals the available grain edge, i.e. a necklace of small grains has formed. Figure 3(b) depicts the evolution of both the average recrystallized grain size $\bar{D}_r$ and the average grain size D_a. Here it can be seen that the average grain size of the smaller grain material (10 and 24 µm initial size) is equal to the recrystallized grain size resulting in an equiaxed grain morphology of grains of average size $\bar{D}_r$.

The model inherently predicts the lack of dependence of the steady state grain size on the initial grain size [7,17,18] which is a widely reported feature of discontinuous dynamic recrystallization. In Figure 3(b) it can be seen that the smaller grain sizes (10 and 24 µm) have more or less converged to the same grain size. The larger initial grain size has a smaller recrystallized grain size, this is due to the fact that the recrystallization is not yet at the steady state. Lastly there is a good match between the recrystallized grain sizes reported by Wahabi et al. and the one predicted by the proposed model. Wahabi measured the recrystallized grain size for the 10, 24 and 92 µm initial grain size experiments to be approximately 5.2, 5 and 3.2 µm, the model is in good agreement with predicted grain sizes of respectively 5.2, 4.9 and 1.9 µm.

In short a physically based model was presented that is able to describe the effect of grain size on the recrystallization behavior. The model predicts not only the effect of recrystallization on the stress–strain response, but also correctly predicts other important microstructural features like recrystallized grain size and morphology aspects like necklacing.

REFERENCES

[1] Sakai, T. and Jonas, J.J, Dynamic Recrystallization: Mechanical and Microstructural considerations, *Acta metall.* Vol. 32 No. 2 (1984) 189-209.

[2] Luton, M.J. and Sellars, C.N. Dynamic recrystallization in nickel and nickel-iron alloys during high temperature deformation, *Acta Metallurgica* Vol 17 (1969) 1033-43.

[3] Misra, R.D.K., Nayak, R.D.K., Mali, S.A., Shah, J.S., Somani, M.C. and Karjalainen, L.P. Microstructure and Deformation Behavior of Phase-Reversion-Induced

Nanograined/Ultrafine-Grained Austenitic Stainless Steel, *Metallurgical and Materials Transactions A*, Vol. 40A (2009) 2498

[4] M.C. Somani, P. Juntunen, L.P. Karjalainen, R.D.K. Misra, A. Kyröläinen, Enhanced Mechanical Properties through Reversion in Metastable Austenitic Stainless Steels, *Metallurgical and Materials Transactions A*, Vol. 40A (2009) 729

[5] Di Schino, A., Barteri, M. and Kenny, J.M Development of ultra fine grain structure by martensitic reversion in stainless steel, *Journal of Materials Science Letters* Vol. 21 (2002) 751-753

[6] Ohadi, D., Parsa, M.H. and Mirzadeh H., Development of dynamic recrystallization maps based on the initial grain size, *Materials Science & Engineering A*, Vol. 565 (2013) 90-95

[7] Wahabi, M. El., Gavard, L., Montheillet, F., Cabrera, J.M. and Prado, J.M. Effect of initial grain size on dynamic recrystallization in high purity austenitic stainless steels, *Acta Materialia*, Vol. 53 (2005) 4605-4612

[8] Humphreys, F.J. and Hatherly, M. *Recrystallization and Related Annealing Phenomena*, second edition, Elsevier Ltd., 2004.

[9] Kooiker, H., Perdahcıoğlu, E.S. and van den Boogaard, A.H. A physically based continuum model for the effect of dynamic recrystallization on the stress–strain response of austenitic stainless steels, submitted

[10] Bergström, Y. 2010, A theory for the temperature and strain-rate dependences of dislocation re-mobilisation, (URL http://www.plastic-deformation.com/paper3.pdf)

[11] Angella, G., Donnini, R., Maldini, M. and Ripamonti, D. Combination between Voce formalism and improved Kocks-Mecking approach to model small strains of flow curves at high temperatures, *Materials Science and Engineering A* 594 (2013) 381-8.

[12] Kooiker, H., Perdahcıoğlu, E.S. and van den Boogaard, A.H. Constitutive modeling of hot forming of austenitic stainless steel 316LN by accounting for recrystallization in the dislocation evolution, *Journal of Physics: Conference Series* Vol. 734 Part B (2016).

[13] Sakai, T., Belyakov, A., Kaibyshev, R., Miura, H. and Jonas, J.J. Dynamic and post-dynamic recrystallization under hot, cold and severe plastic deformation conditions, *Progress in Materials Science*, Vol. 60 (2014) 130-207

[14] Hoseini Asli, A. and Zarei-Hanzaki, A. Dynamic Recrystallization Behavior of a Fe-Cr-Ni Super-Austenitic Stainless Steel, *J. Mater. Sci. Technol.* Vol. 25 No. 5 (2009) 603-606

[15] Tikhonova, M., Dolzhenko, P., Kaibyshev, R. and Belyakov, A. Grain Boundary Assemblies in Dynamically-Recrystallized Austenitic Stainless Steels, *Metals* (2016)

[16] Doherty, R.D., Hughes, D.A., Humphreys, F.J., Jonas, J.J., Juul Jensen, D., Kassner, M.E., King, W.E., McNelley, T.R., McQueen, H.J. and Rollet A.D., Current issues in recrystallization: a review, *Materials Science and Engineering* A 238 (1997) 219-74.

[17] Takigawa, Y., Honda, M., Uesughi, T. and Higashi, K. Effect of Initial Grain Size on Dynamically Recrystallized Grain Size in AZ31 Magnesium Alloy, *Materials Transactions*, Vol. 49 No. 9 (2008) 1979-1982

[18] Zhao, D. and Chaudbury, P.K. Effect of starting grain size on as-deformed microstructure in high temperature deformation of alloy 718, *The minerals, Metals & Materials Society*, (1994) 303-313
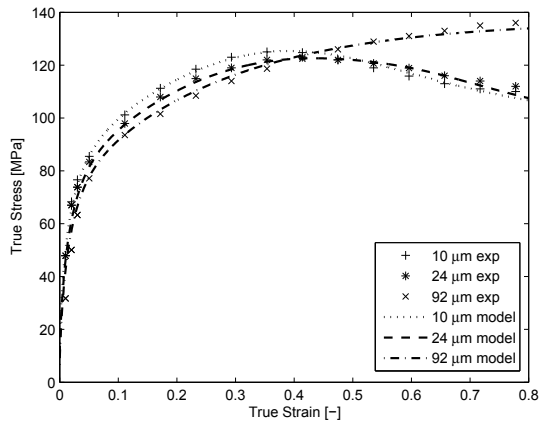
(a) Stress–strain response, experimental and simulation
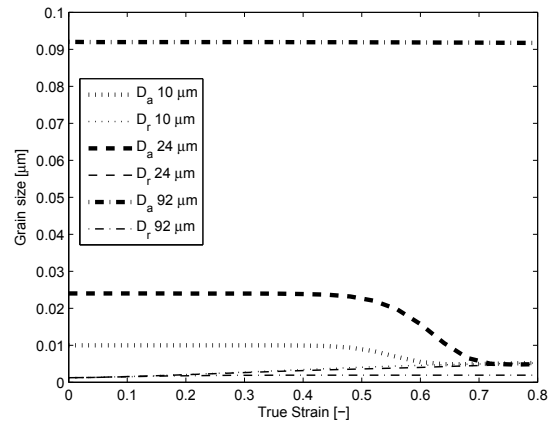
(b) Simulation of the evolution of the recrystallized grain size $\bar{D}_r$ and overall grain size D_a
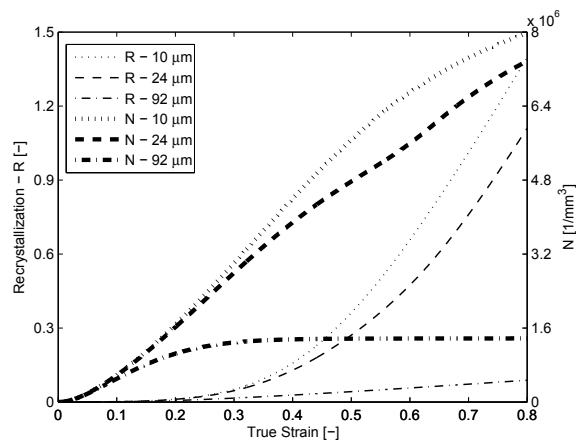
(c) Simulation of the evolution of the recrystallization and number of actively recrystallizing grains

Figure 3: Selected experimental and model results for initial grain sizes 10, 24 and 92 µm